

# Spin-orbit torques in high-resistivity-W/CoFeB/MgO


著者	Yutaro Takeuchi, Chaoliang Zhang, Atsushi Okada, Hideo Sato, Shunsuke Fukami, Hideo Ohno
journal or publication title	Applied Physics Letters
volume	112
number	19
page range	192408
year	2018-05-07
URL	<a href="http://hdl.handle.net/10097/00128252">http://hdl.handle.net/10097/00128252</a>

doi: 10.1063/1.5027855

# Spin-orbit torques in high-resistivity-W/ CoFeB/MgO

Cite as: Appl. Phys. Lett. **112**, 192408 (2018); <https://doi.org/10.1063/1.5027855>

Submitted: 06 March 2018 . Accepted: 26 April 2018 . Published Online: 10 May 2018

Yutaro Takeuchi, Chaoliang Zhang, Atsushi Okada, Hideo Sato , Shunsuke Fukami, and Hideo Ohno



View Online



Export Citation



CrossMark

## ARTICLES YOU MAY BE INTERESTED IN

[Spin transfer torque devices utilizing the giant spin Hall effect of tungsten](#)

Applied Physics Letters **101**, 122404 (2012); <https://doi.org/10.1063/1.4753947>

[Recent advances in spin-orbit torques: Moving towards device applications](#)

Applied Physics Reviews **5**, 031107 (2018); <https://doi.org/10.1063/1.5041793>

[Size dependence of the spin-orbit torque induced magnetic reversal in W/CoFeB/MgO nanostructures](#)

Applied Physics Letters **112**, 142410 (2018); <https://doi.org/10.1063/1.5022824>

Lock-in Amplifiers  
up to 600 MHz



Watch



## Spin-orbit torques in high-resistivity-W/CoFeB/MgO

Yutaro Takeuchi,<sup>1</sup> Chaoliang Zhang,<sup>1,2,3</sup> Atsushi Okada,<sup>1</sup> Hideo Sato,<sup>1,3,4,5</sup> Shunsuke Fukami,<sup>1,3,4,5,a)</sup> and Hideo Ohno<sup>1,3,4,5,6</sup>

<sup>1</sup>Laboratory for Nanoelectronics and Spintronics, Research Institute of Electrical Communication, Tohoku University, Sendai 980-8577, Japan

<sup>2</sup>Frontier Research Institute for Interdisciplinary Sciences, Tohoku University, Sendai 980-8578, Japan

<sup>3</sup>Center for Spintronics Integrated Systems, Tohoku University, Sendai 980-8577, Japan

<sup>4</sup>Center for Innovative Integrated Electronic Systems, Tohoku University, Sendai 980-8572, Japan

<sup>5</sup>Center for Spintronics Research Network, Tohoku University, Sendai 980-8577, Japan

<sup>6</sup>WPI-Advanced Institute for Materials Research (WPI-AIMR), Tohoku University, Sendai 980-8577, Japan

(Received 6 March 2018; accepted 26 April 2018; published online 10 May 2018)

Magnetic heterostructures consisting of high-resistivity ( $238 \pm 5 \mu\Omega \text{ cm}$ )-W/CoFeB/MgO are prepared by sputtering and their spin-orbit torques are evaluated as a function of W thickness through an extended harmonic measurement. W thickness dependence of the spin-orbit torque with the Slonczewski-like symmetry is well described by the drift-diffusion model with an efficiency parameter, the so-called effective spin Hall angle, of  $-0.62 \pm 0.03$ . In contrast, the field-like spin-orbit torque is one order of magnitude smaller than the Slonczewski-like torque and shows no appreciable dependence on the W thickness, suggesting a different origin from the Slonczewski-like torque. The results indicate that high-resistivity W is promising for low-current and reliable spin-orbit torque-controlled devices. *Published by AIP Publishing.*

<https://doi.org/10.1063/1.5027855>

The in-plane current flowing into magnetic heterostructures has been found to give rise to torques, spin-orbit torques (SOTs), acting upon the magnetization as a consequence of the spin-orbit interaction, such as the spin Hall effect (SHE)<sup>1,2</sup> and the Rashba-Edelstein effect.<sup>3,4</sup> Recent studies have shown that the SOT accomplishes efficient magnetization switching,<sup>5-7</sup> and is recognized as a key ingredient for high-performance spintronic memory devices.<sup>8</sup> The SOT has two vector components with different symmetries, namely, the Slonczewski-like (SL) torque with  $\mathbf{m} \times (\mathbf{m} \times \boldsymbol{\sigma})$  symmetry and the field-like (FL) torque with  $\mathbf{m} \times \boldsymbol{\sigma}$  symmetry, where  $\mathbf{m}$  is the unit vector of magnetization and  $\boldsymbol{\sigma}$  is the spin accumulation vector. The efficiency of SOT generation under a given current density  $J$  is characterized by dimensionless parameters<sup>9</sup>

$$\zeta_{\text{SL(FL)}} = \frac{2eH_{\text{SL(FL)}}m_S}{\hbar J}, \quad (1)$$

where  $e$  is the electron charge,  $H_{\text{SL(FL)}}$  the effective fields of SL(FL) torques,  $m_S$  the spontaneous magnetic moment per unit area, and  $\hbar$  the Dirac constant.  $\zeta_{\text{SL}}$  corresponds to the effective spin Hall angle  $\theta_{\text{SH}}^{\text{eff}}$ , in case the SL torque originates from a bulk SHE inside a layer with its thickness sufficiently greater than the spin diffusion length. A large  $\zeta_{\text{SL}}$  is desirable to achieve a small critical current for SOT-induced magnetization switching. Up to now, a relatively large  $\zeta_{\text{SL}}$  has been reported for heterostructures with Pt,<sup>5,9-12</sup> Ta,<sup>6,7,12-14</sup> W,<sup>12,15-21</sup> Hf,<sup>16,22,23</sup> PtMn,<sup>24,25</sup> and so on.<sup>26-30</sup> Among them, W is a leading candidate for applications due to the large  $\zeta_{\text{SL}}$  of  $-0.2$  to  $-0.5$ . It was also found that  $\zeta_{\text{SL}}$  can be enhanced by increasing the W resistivity in the range of  $100$ – $200 \mu\Omega \text{ cm}$ .<sup>20</sup> Thus, the first focus of this study is to examine whether  $\zeta_{\text{SL}}$  can be further enhanced

by increasing the W resistivity. Meanwhile, the FL torque in systems with W has not been investigated well. The FL torque was also found to effectively reduce the critical current in nanoscale devices<sup>31</sup> and also govern the spatial evolution of magnetization switching in sub-micrometer-scale devices;<sup>32</sup> however, a recent study pointed out that it could cause switching-back events through a domain wall reflection at the sample edge.<sup>33</sup> Thus, the quantification of the FL torque for heterostructures with W is of equal importance and is the second focus of this work. In addition to the above, the origin of SL and FL torques has been a long-standing debatable issue and is also addressed in this work. To this end, here, we prepare W/CoFeB/MgO heterostructures, where W has various thicknesses and has a higher resistivity than previous studies. We evaluate both components of SOT by the extended harmonic Hall resistance measurement.<sup>34,35</sup> The thickness of CoFeB is designed to show an in-plane easy axis because of its promising potential for high-speed memory applications<sup>36,37</sup> and capability to exclude non-negligible thermoelectric effects by analysis.<sup>34,35</sup>

All the samples are deposited on thermally oxidized Si substrates by DC/RF magnetron sputtering using Ar as an inert gas. The stacks consist of, from the substrate side, W( $t_W$ )/CoFeB(2.0)/MgO(1.3)/Ta(1). Nominal thicknesses in nm indicated as the numbers in parentheses are controlled by the deposition time based on the deposition rates of each material, which are confirmed by X-ray reflectivity measurements. The deposition conditions of W, especially the Ar gas pressure during the sputtering is tuned, so that the W layer shows high resistivity. The actual Ar gas pressure in the deposition chamber is  $0.25 \text{ Pa}$  and the deposition rate of W is  $0.010 \text{ nm/s}$ . The W thickness  $t_W$  is varied in the range of  $1$ – $6 \text{ nm}$ . Magnetization curves of blanket films are evaluated with a vibrating sample magnetometer, from which  $m_S$  is determined to be  $2.44 \pm 0.09 \text{ T nm}$ . The stacks are processed into Hall bar devices with the

<sup>a)</sup>Author to whom correspondence should be addressed: s-fukami@riec.tohoku.ac.jp. Telephone: +81-22-217-5554. Fax: +81-22-217-5555.

channel size of  $10 \times 50 \mu\text{m}^2$  by photolithography and Ar ion milling. The effective fields of SL and FL SOTs are evaluated from the extended harmonic Hall resistance measurement, which is capable of excluding the thermoelectric effects originating from the anomalous Nernst and spin Seebeck effects.<sup>34,35</sup> The schematic diagram of the measurement setup is shown in Fig. 1(a). An in-plane external magnetic field  $H_{\text{ext}}$  with various magnitudes is rotated in the film plane, whose direction is represented by the azimuthal angle  $\phi_H$ . 10-Hz AC is applied to the channel and the first and second harmonic Hall voltages are measured by a lock-in amplifier. All measurements are conducted at room temperature.

We first evaluate the resistivity of each layer of the deposited stacks. To quantify the W resistivity  $\rho_W$ , the channel resistance of Hall bar devices with various  $t_W$  is measured and the conductance is plotted as a function of  $t_W$ , as shown in Fig. 1(b).  $\rho_W$  is obtained to be  $238 \pm 5 \mu\Omega \text{cm}$  from the slope. The intercept represents the conductance of a CoFeB layer. MgO and top Ta layers are found to be insulating. From the obtained  $\rho_W$  and the total channel conductance, the current density  $J_W$  flowing into the W layer is calculated for each  $t_W$ .

We then evaluate the SOT using the Hall devices. The out-of-plane magnetic field ( $H_Z$ ) dependence of the Hall resistance ( $R_{\text{Hall}}$ ) is first measured to quantify the saturation value of the anomalous Hall resistance  $R_{\text{AHE}}$  and the effective perpendicular magnetic anisotropy field  $H_K^{\text{eff}}$ , which are necessary to analyze the SOT. Figure 1(c) shows a  $R_{\text{Hall}}$  vs.  $H_Z$  curve in the Hall device with  $t_W = 1 \text{ nm}$ . The result shows a typical behavior when a magnetic field is applied along the hard axis, indicating that the fabricated device has an in-plane magnetic easy axis. In this configuration, the ordinary Hall effect (OHE) and the anomalous Hall effect (AHE) contribute to  $R_{\text{Hall}}$ .  $R_{\text{AHE}}$  is determined from the intercept on the vertical axis of the linear fit to the data in high-field regimes (red lines), in which magnetization saturates to the out-of-plane direction and  $R_{\text{Hall}}$  originates in only OHE.  $H_K^{\text{eff}}$  is determined from the  $x$ -component of

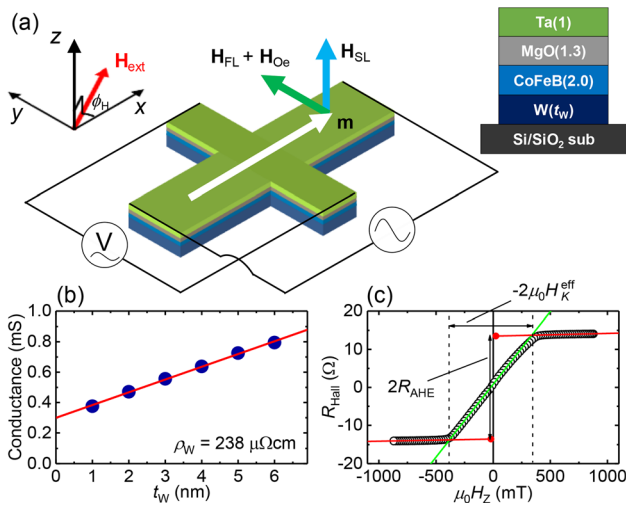


FIG. 1. (a) Schematic of the measurement configuration for evaluating the SOT with the coordinate system. (b) Channel conductance of Hall bar vs. W thickness  $t_W$ . The red line denotes a linear fit. (c) Out-of-plane magnetic field  $H_Z$  dependence of Hall resistance  $R_{\text{Hall}}$  for the W(1)/CoFeB(2.0)/MgO/Ta(1) Hall bar device measured with the channel current of 100  $\mu\text{A}$ .  $\mu_0$  is the permeability in free space. Black plots, red lines, and the green line denote the experimental data, linear fits in high-field regimes and that in the low-field regime, respectively.

intersection between the linear fits in the high-field regimes and a linear fit in the low-field regime (green line) where magnetization is raised from the in-plane direction by  $H_Z$  and  $R_{\text{Hall}}$  originates in both OHE and AHE. The obtained  $\mu_0 H_K^{\text{eff}}$  is  $-360$  to  $-400 \text{ mT}$  and has no clear trend with respect to  $t_W$ , whereas  $R_{\text{AHE}}$  monotonically decreases with increasing  $t_W$  due to a reduction of current flowing into the CoFeB layer.

Figures 2(a) and 2(b), respectively, show the first ( $R_{\omega}$ ) and second ( $R_{2\omega}$ ) harmonic Hall resistances as a function of  $\phi_H$  for various  $t_W$ . Because CoFeB used in this study has an in-plane easy axis,  $R_{\omega}$  is dominated by the planar Hall resistance and thus is represented as<sup>34,35</sup>

$$R_{\omega} = R_{\text{PHE}} \sin 2\phi, \quad (2)$$

where  $R_{\text{PHE}}$  is the planar Hall resistance coefficient and  $\phi$  the azimuthal angle of magnetization from the  $x$  axis. In the Hall bar structure, the in-plane anisotropy is negligibly small, and one can expect that the magnetization follows the magnetic field ( $\phi = \phi_H$ ). We confirm that this is indeed the case by the fit of Eq. (2) to the results with  $\phi = \phi_H$  [black lines in Fig. 2(a)], which reproduces well the experimental results.  $R_{2\omega}$  is subject to the current-induced effective fields and its dependence on  $\phi$  is described by<sup>34,35</sup>

$$R_{2\omega} = - \left( R_{\text{AHE}} \frac{H_{\text{SL}}}{H_{\text{ext}} - H_K^{\text{eff}}} + R_T \right) \cos \phi + 2R_{\text{PHE}} \frac{H_{\text{FL}} + H_{\text{Oe}}}{H_{\text{ext}}} (2 \cos^3 \phi - \cos \phi), \quad (3)$$

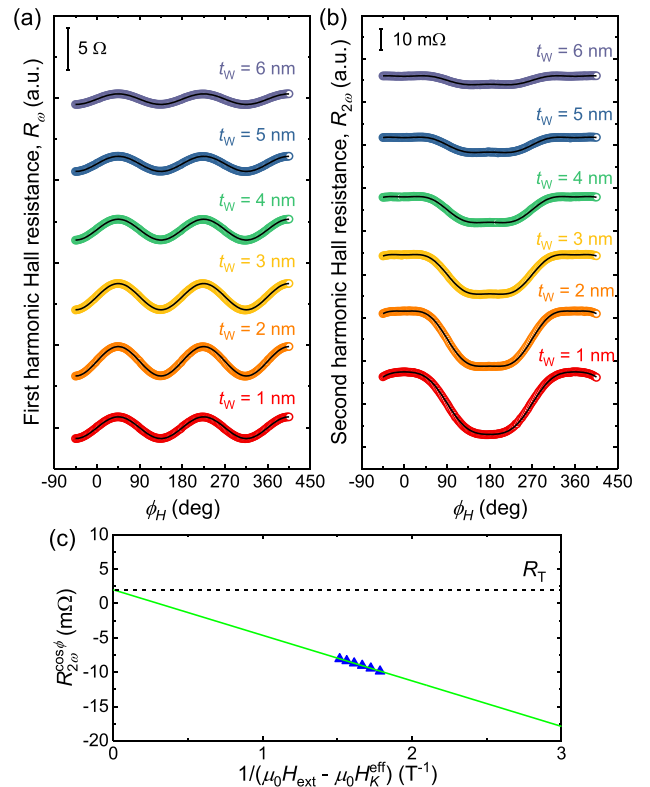


FIG. 2. In-plane magnetic field angle  $\phi_H$  dependence of harmonic Hall resistance (a)  $R_{\omega}$  and (b)  $R_{2\omega}$  with various W thicknesses  $t_W$ . AC of 1.5 mA and an in-plane magnetic field of 300 mT are applied. The black curves are fitting with Eqs. (2) and (3). (c) The  $\cos \phi$  contribution of the second harmonic Hall resistance  $R_{2\omega}^{\cos \phi}$  as a function of  $1/(\mu_0 H_{\text{ext}} - \mu_0 H_K^{\text{eff}})$  for  $t_W = 4 \text{ nm}$ . The green line denotes the linear fit.

where  $R_T$  is the second harmonic Hall resistance coefficient due to the thermo-electric voltage and  $H_{Oe}$  the current-induced Oersted field. The thermo-electric voltage originates from the anomalous Nernst and spin Seebeck effects.<sup>34,35</sup> The measured  $R_{2\omega}$  vs.  $\phi_H$  is separated into  $\cos\phi$  and  $2\cos^3\phi - \cos\phi$  contributions by fitting with Eq. (3) and  $\phi = \phi_H$ .  $H_{SL}$  and  $R_T$  can be distinguished by evaluating the  $H_{ext}$  dependence of  $\cos\phi$  contribution. Figure 2(c) shows the  $\cos\phi$  contribution of  $R_{2\omega}$  ( $R_{2\omega}^{\cos\phi}$ ) as a function of  $1/(H_{ext} - H_K^{\text{eff}})$ .  $H_{SL}$  and  $R_T$  are obtained from the slope and the y-intercept of the linear fit, respectively.  $H_{FL} + H_{Oe}$  is determined from the  $2\cos^3\phi - \cos\phi$  contribution at  $\mu_0 H_{ext} = 300$  mT, which is the maximum external field in our experimental setup. As the width of the Hall bar ( $10\ \mu\text{m}$ ) is much larger than the film thickness,  $H_{Oe}$  is calculated from a simplified Ampere's law:  $H_{Oe} = I_W/2w$ , where  $I_W$  is the current flowing into the W layer and  $w$  is the channel width.<sup>28</sup>

Figures 3(a) and 3(b), respectively, show the obtained  $H_{SL}$  and  $H_{FL}$  as a function of  $J_W$  for a device with  $t_W = 4$  nm. Both  $H_{SL}$  and  $H_{FL}$  are proportional to the applied current, proving that  $H_{SL}$  and  $H_{FL}$  are induced by the current. The calculated  $H_{Oe}$  is also shown as a violet solid line in Fig. 3(b), which has the same sign as that of  $H_{FL}$ , but much smaller in magnitude. Figures 3(c) and 3(d) show the  $t_W$  dependence of  $\zeta_{SL}$  and  $\zeta_{FL}$ , respectively, calculated from Eq. (1) using the obtained  $H_{SL}$  and  $H_{FL}$  shown in Figs. 3(a) and 3(b) and  $m_S$  measured with a vibrating sample magnetometer. It is found that  $\zeta_{SL}$  increases and converges to a certain value as  $t_W$  increases. As described earlier, in case that  $H_{SL}$  originates from the bulk SHE,  $\zeta_{SL}$  is described by the drift-diffusion model<sup>10</sup>

$$\zeta_{SL} = \theta_{SH}^{\text{eff}} \left( 1 - \text{sech} \left( \frac{t_W}{\lambda_{sf}} \right) \right), \quad (4)$$

where  $\lambda_{sf}$  is the spin diffusion length of W. Fitting Eq. (4) to  $t_W$  dependence of  $\zeta_{SL}$  leads to  $\theta_{SH}^{\text{eff}} = -0.62 \pm 0.03$  and  $\lambda_{sf} = 1.31 \pm 0.08$  nm. The obtained  $\theta_{SH}^{\text{eff}}$  is the highest value among previous studies on heterostructures with W.<sup>12,15–21</sup> We note that  $\theta_{SH}^{\text{eff}}$  of W with a lower resistivity of  $200\ \mu\Omega\ \text{cm}$ , deposited at the Ar gas pressure of  $0.19$  Pa, is determined to

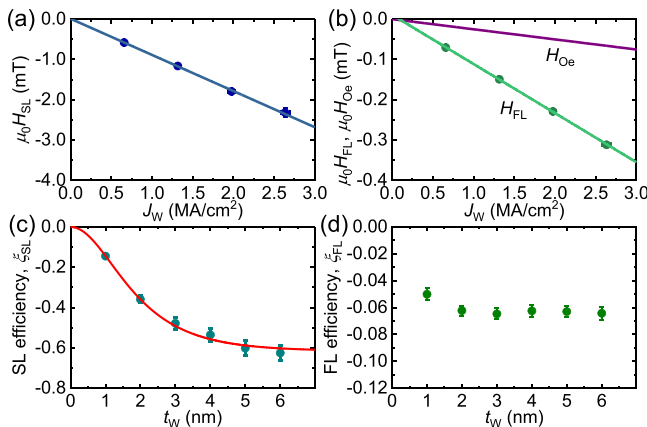


FIG. 3. Current-induced effective fields (a)  $H_{SL}$  and (b)  $H_{FL}$  as a function of current density  $J_W$  flowing into the W layer for  $t_W = 4$  nm. The violet solid line in (b) shows the Oersted field  $H_{Oe}$ . W thickness  $t_W$  dependence of (c)  $\zeta_{SL}$  and (d)  $\zeta_{FL}$ . The red solid line denotes the fitting curve based on the drift-diffusion model [Eq. (4)].

be  $-0.47 \pm 0.05$  with  $\lambda_{sf} = 1.33 \pm 0.08$  nm by the same method, in agreement with previous results on W with similar resistivity,<sup>18,20</sup> indicating the validity of the employed procedure. Therefore, the obtained large  $\zeta_{SL}$  can be attributed to the highly resistive W that exhibits a strong SHE. The increase in  $\zeta_{SL}$  also suggests that the intrinsic mechanism or side-jump scattering are more likely to be responsible for the SHE than skew scattering, since  $\zeta_{SL}$  is known to be proportional to (constant with) the longitudinal resistivity for the former (latter).<sup>38</sup> In contrast,  $\zeta_{FL}$  shows no significant dependence on  $t_W$ . This suggests that the origin of FL torque is different from the SL torque and can be attributed to the spin-orbit interaction at the interface such as the Rashba-Edelstein effect. A similar result was reported in systems with Pd/Co/AIO<sub>x</sub>.<sup>30</sup> It is also notable that  $\zeta_{FL}$  is one order of magnitude smaller than  $\zeta_{SL}$ , which agrees with an implication in a previous study on SOT-induced magnetization switching.<sup>20</sup> Such a small magnitude of  $\zeta_{FL}$  relative to  $\zeta_{SL}$  is in stark contrast to the cases with Pt/Co/AIO<sub>x</sub><sup>11</sup> and Ta/CoFeB/MgO<sup>13,14</sup> heterostructures. In addition, if the FL torque can cause switching-back events,<sup>33</sup> the present W/CoFe/MgO with a small  $\zeta_{FL}$  and a large  $\zeta_{SL}$  is promising to achieve low-current and reliable magnetization switching. We also note that recent studies pointed out that the FL torque quickly decays with an increase in the ferromagnetic layer thickness due to the rotation of spin current away from the spin-accumulation axis.<sup>34,39</sup> In this case, the FL torque could increase when one uses perpendicular-easy-axis systems with a thinner ferromagnetic layer.

In summary, we investigate W thickness dependence of SOTs in high-resistivity ( $238 \pm 5\ \mu\Omega\ \text{cm}$ )-W/CoFeB/MgO using an extended harmonic Hall resistance measurement. W thickness dependence of Slonczewski-like SOT is well described by the drift-diffusion model that assumes bulk SHE as an origin of SOT. The effective spin Hall angle is derived to be  $-0.62 \pm 0.03$ ; the highest value among the studies on metallic tri-layer systems reported so far. Field-like SOT, on the other hand, is one order of magnitude smaller than the Slonczewski-like SOT. No appreciable dependence of the field-like SOT on W thickness is observed, suggesting interfacial spin-orbit interactions as the origin. The obtained results indicate that heterostructures with high-resistivity W is promising for low-current and high-reliability SOT-controlled devices.

The authors thank T. Hirata, H. Iwanuma, K. Goto, and C. Igarashi for their technical support. A portion of this work was supported by the ImPACT Program of CSTI, JST-OPERA, JSPS KAKENHI Grant No. 17H06093, JSPS Core-to-Core Program, and RIEC Cooperative Research Projects. Y.T. acknowledges the Graduate Program in Spintronics, Tohoku University.

<sup>1</sup>M. I. D'yakonov and V. I. Perel, *Phys. Lett. A* **35**, 459 (1971).

<sup>2</sup>J. E. Hirsch, *Phys. Rev. Lett.* **83**, 1834 (1999).

<sup>3</sup>E. I. Rashba, *Fiz. Tverd. Tela (Leningrad)* **2**, 1224 (1960) [*Sov. Phys. Solid State* **2**, 1109 (1960)].

<sup>4</sup>V. M. Edelstein, *Solid State Commun.* **73**, 233 (1990).

<sup>5</sup>I. M. Miron, K. Garello, G. Gaudin, P. J. Zermatten, M. V. Costache, S. Auffret, S. Bandiera, B. Rodmacq, A. Schuhl, and P. Gambardella, *Nature* **476**, 189 (2011).

<sup>6</sup>L. Liu, C.-F. Pai, Y. Li, H. W. Tseng, D. C. Ralph, and R. A. Buhrman, *Science* **336**, 555 (2012).

<sup>7</sup>S. Fukami, T. Anekawa, C. Zhang, and H. Ohno, *Nat. Nanotechnol.* **11**, 621 (2016).

- <sup>8</sup>S. Fukami and H. Ohno, *Jpn. J. Appl. Phys., Part 1* **56**, 0802A1 (2017).
- <sup>9</sup>C.-F. Pai, Y. Ou, L. Henrique, L. H. Vilela-Leão, D. C. Ralph, and R. A. Buhrman, *Phys. Rev. B* **92**, 064426 (2015).
- <sup>10</sup>L. Liu, T. Moriyama, D. C. Ralph, and R. A. Buhrman, *Phys. Rev. Lett.* **106**, 036601 (2011).
- <sup>11</sup>K. Garello, I. M. Miron, C. O. Avci, F. Freimuth, Y. Mokrousov, S. Blügel, S. Auffret, O. Boulle, G. Gaudin, and P. Gambardella, *Nat. Nanotechnol.* **8**, 587 (2013).
- <sup>12</sup>C. O. Avci, K. Garello, J. Mendil, A. Ghosh, N. Blasakis, M. Gabureac, M. Trassin, M. Fiebig, and P. Gambardella, *Appl. Phys. Lett.* **107**, 192405 (2015).
- <sup>13</sup>J. Kim, J. Sinha, M. Hayashi, M. Yamanouchi, S. Fukami, T. Suzuki, S. Mitani, and H. Ohno, *Nat. Mater.* **12**, 240 (2013).
- <sup>14</sup>C. Zhang, M. Yamanouchi, H. Sato, S. Fukami, S. Ikeda, F. Matsukura, and H. Ohno, *Appl. Phys. Lett.* **103**, 262407 (2013).
- <sup>15</sup>C.-F. Pai, L. Liu, Y. Li, H. W. Tseng, D. C. Ralph, and R. A. Buhrman, *Appl. Phys. Lett.* **101**, 122404 (2012).
- <sup>16</sup>C.-F. Pai, M.-H. Nguyen, C. Belvin, L. H. Vilela-Leão, D. C. Ralph, and R. A. Buhrman, *Appl. Phys. Lett.* **104**, 082407 (2014).
- <sup>17</sup>S. Cho, S.-H. C. Baek, K.-D. Lee, Y. Jo, and B.-G. Park, *Sci. Rep.* **5**, 14668 (2015).
- <sup>18</sup>K.-U. Demasius, T. Phung, W. Zhang, B. P. Hughes, S.-H. Yang, A. Kellock, W. Han, A. Pushp, and S. S. P. Parkin, *Nat. Commun.* **7**, 10644 (2016).
- <sup>19</sup>L. Neumann, D. Meier, J. Schmalhorst, K. Rott, G. Reiss, and M. Meinert, *Appl. Phys. Lett.* **109**, 142405 (2016).
- <sup>20</sup>C. Zhang, S. Fukami, K. Watanabe, A. Ohkawara, S. DuttaGupta, H. Sato, F. Matsukura, and H. Ohno, *Appl. Phys. Lett.* **109**, 192405 (2016).
- <sup>21</sup>S. Mondal, S. Choudhury, N. Jha, A. Ganguly, J. Sinha, and A. Barman, *Phys. Rev. B* **96**, 054414 (2017).
- <sup>22</sup>M. Akyol, G. Yu, J. G. Alzate, P. Upadhyaya, X. Li, K. L. Wong, A. Ekicibil, P. K. Amiri, and K. L. Wang, *Appl. Phys. Lett.* **106**, 162409 (2015).
- <sup>23</sup>M. Akyol, W. Jiang, G. Yu, Y. Fan, M. Gunes, A. Ekicibil, P. K. Amiri, and K. L. Wang, *Appl. Phys. Lett.* **109**, 022403 (2016).
- <sup>24</sup>W. Zhang, M. B. Jungfleisch, W. Jiang, J. E. Pearson, A. Hoffmann, F. Freimuth, and Y. Mokrousov, *Phys. Rev. Lett.* **113**, 196602 (2014).
- <sup>25</sup>S. Fukami, C. Zhang, S. DuttaGupta, A. Kurenkov, and H. Ohno, *Nat. Mater.* **15**, 535 (2016).
- <sup>26</sup>Y. Niimi, Y. Kawanishi, D. H. Wei, C. Deranlot, H. X. Yang, M. Chshiev, T. Valet, A. Fert, and Y. Otani, *Phys. Rev. Lett.* **109**, 156602 (2012).
- <sup>27</sup>W. Zhang, M. B. Jungfleisch, F. Freimuth, W. Jiang, J. Sklenar, J. E. Pearson, J. B. Ketterson, Y. Mokrousov, and A. Hoffman, *Phys. Rev. B* **92**, 144405 (2015).
- <sup>28</sup>V. Tshitoyan, C. Ciccirelli, A. P. Mihai, A. C. Irvine, T. A. Moore, T. Jungwirth, and A. J. Ferguson, *Phys. Rev. B* **92**, 214406 (2015).
- <sup>29</sup>Y.-W. Oh, S.-H. C. Beak, Y. M. Kim, H. Y. Lee, K.-D. Lee, C.-G. Yang, E.-S. Park, K.-S. Lee, K.-W. Kim, G. Go, J.-R. Jeong, B.-C. Min, H.-W. Lee, K.-J. Lee, and B.-G. Park, *Nat. Nanotechnol.* **11**, 878 (2016).
- <sup>30</sup>A. Ghosh, K. Garello, C. O. Avci, M. Gabureac, and P. Gambardella, *Phys. Rev. Appl.* **7**, 014004 (2017).
- <sup>31</sup>C. Zhang, S. Fukami, H. Sato, F. Matsukura, and H. Ohno, *Appl. Phys. Lett.* **107**, 012401 (2015).
- <sup>32</sup>M. Baumgartner, K. Garello, J. Mendil, C. O. Avci, E. Grimaldi, C. Murer, J. Feng, M. Gabureac, C. Stamm, Y. Acremann, S. Finizio, S. Wintz, J. Raabe, and P. Gambardella, *Nat. Nanotechnol.* **12**, 980 (2017).
- <sup>33</sup>J. Yoon, S.-W. Lee, J. H. Kwon, J. M. Lee, J. Son, X. Qiu, K.-J. Lee, and H. Yang, *Sci. Adv.* **3**, e1603099 (2017).
- <sup>34</sup>C. O. Avci, K. Garello, M. Gabureac, A. Ghosh, A. Fuhrer, S. F. Alvarado, and P. Gambardella, *Phys. Rev. B* **90**, 224427 (2014).
- <sup>35</sup>Y.-C. Lau and M. Hayashi, *Jpn. J. Appl. Phys., Part 1* **56**, 0802B5 (2017).
- <sup>36</sup>S. Fukami, T. Anekawa, A. Ohkawara, C. Zhang, and H. Ohno, in *VLSI Symposia* (2016), p. T06-05.
- <sup>37</sup>S. Shi, Y. Ou, S. V. Aradya, D. C. Ralph, and R. A. Buhrman, *Phys. Rev. Appl.* **9**, 011002 (2018).
- <sup>38</sup>A. Hoffman, *IEEE Trans. Magn.* **49**, 5172 (2013).
- <sup>39</sup>T. D. Skinner, M. Wang, A. T. Hindmarch, A. W. Rushforth, A. C. Irvine, D. Heiss, H. Kurebayashi, and A. J. Ferguson, *Appl. Phys. Lett.* **104**, 062401 (2014).